

Attosecond imaging of photo-induced dynamics in molecules using time-resolved photoelectron momentum microscopy

Marvin Reuner¹, Daria Popova-Gorelova^{1,2}

¹*I. Institute for Theoretical Physics and Centre for Free-Electron Laser Science, Universität Hamburg, Notkestraße 9, 22607 Hamburg, Germany*

²*The Hamburg Centre for Ultrafast Imaging (CUI), Luruper Chaussee 149, 22607 Hamburg, Germany*

(Dated: January 18, 2023)

We explore the novel capabilities offered by attosecond extreme ultraviolet and x-ray pulses that can be now generated by free-electron lasers and high-harmonics generation sources for probing photon-induced electron dynamics in molecules. We theoretically analyze how spatial and temporal dependence of charge migration in a pentacene molecule can be followed by means of time-resolved photoelectron microscopy on the attosecond time scale. Performing the analysis, we accurately take into account that an attosecond probe pulse leads to considerable spectral broadening. We demonstrate that the excited-state dynamics of a neutral pentacene molecule in the real space map onto unique features of photoelectron momentum maps.

I. INTRODUCTION

Photoelectron momentum microscopy is the technique, in which a light pulse ionizes a probe leading to the detachment of a photoelectron. The momentum distribution of the detached photoelectron encodes information about the shape of an orbital or a bond in the real space from which the electron was detached [1–12]. This connection is facilitated by the Fourier transform, which links the real and momentum space. The spatial resolution of this technique is given by the de-Broglie wavelength of the emitted photoelectron, which is determined by the kinetic energy of the photoelectron. If an extreme ultraviolet (XUV) probe pulse detaches an electron from a valence orbital, the photoelectron would also have a kinetic energy in the XUV range corresponding to the resolution of a few Angstroms.

In recent years, there has been a remarkable progress in atomic-scale imaging of photo-excited states and dynamics using photoelectron momentum microscopy. Momentum-space distribution of transiently excited electrons was measured [13], the dynamics of crystalline bonds have been followed during the photo-induced phase transition [9] and the technique allowed to detect singlet fission with orbital resolution [14]. Time-resolved photoelectron momentum microscopy probing photo-induced dynamics of pentacene films on sub-picosecond time scale has been achieved at the free-electron laser FLASH [15]. So far, these experiments were performed at a sub-picosecond time scale and were not capable of capturing pure electron dynamics in real time on its natural time scale. This barrier is now feasible to overcome due to the new capabilities to produce attosecond x-ray pulses at free-electron lasers [16–18] or attosecond XUV pulses using high-harmonics generation sources [19–25]. These sources have already been successfully employed to study electronic processes with few-femtosecond to attosecond time and atomic-scale space resolution [26–36], and new experimental schemes are being explored theoretically

[37–49]. The interpretation of a signal from attosecond probe pulses is challenging, since they have a broad bandwidth in the energy domain, which smears out spectral lines in a signal. In this article, we analyze how attosecond XUV pulses can be employed to measure charge migration in a pentacene molecule and analyze how to extract the real-space and real-time information about charge migration using the momentum-resolved photoelectron microscopy.

Pentacene is a prototypical organic semiconductor composed of pentacene molecules, which is among candidate materials for efficient organic photovoltaics [50, 51]. The understanding of the process of solar-energy conversion in organic semiconductors strongly relies on the insight into both intra- and intermolecular photo-excited processes [52]. Exciton migration is one of the fundamental processes governing solar-energy conversion and the role of electronic coherence processes becomes especially relevant near conical intersections [53–55]. Electronic charge-migration dynamics launched as a coherent superposition of electronic states have already been studied in detail [56–65]. In this paper, we focus on the description of how such coherent electron dynamics can be probed on nanoscale by broadband probe pulses. Particularly, we study how attosecond photoelectron momentum microscopy can be employed to probe intramolecular coherent exciton dynamics in pentacene.

It has been shown that time-resolved photoelectron spectroscopy can be applied to probe ultrafast electronic and nuclear molecular dynamics [43, 66–71]. However, angle-unresolved photoelectron spectra do not carry any spatial information about the dynamics, which is lost due to angle averaging. In photoelectron momentum microscopy, momentum distribution of photoelectrons is detected. The great advantage of this technique over angle-averaged spectroscopy is that the distribution provides details of electron dynamics within a molecule, if photoelectrons are detached with high kinetic energies. We will also show that photoelectron spectra can lose

important time-resolved information about the dynamics after angle averaging.

In this article, we apply the general theoretical formalism to describe the time and momentum-dependend photoelectron probability by a broad-bandwidth probe pulse derived in Ref. [7]. That study proposed to probe hole dynamics in a positively ionized molecule by emitting electrons from orbitals that were initially occupied. Here, we propose to apply attosecond XUV pulses to probe photoexcited states of a neutral molecule, which is especially relevant to reveal information about exciton dynamics in the energy conversion processes.

The article is organized as follows. We develop the theoretical description of time-resolved photoelectron momentum microscopy of excited-state dynamics in molecules taking electron correlations and broad-bandwidth of a probe pulse into account in Sec. II. In Sec. III, we calculate photoelectron spectra and photoelectron momentum maps from coherent electron-hole dynamics in a pentacene molecule obtained by an attosecond XUV probe pulse. We reveal how time-resolved atomic-scale changes in electron density are correlated with time-resolved changes in photoelectron momentum maps.

II. METHOD

Throughout this article, we consider a molecule with coherently evolving electron dynamics. In this case, the N_{el} -electron wave function of a molecule is a coherent superposition of several excited electronic eigenstates $|\Phi_I\rangle$

$$|\Psi(t)\rangle = \sum_I C_I e^{-iE_I(t-t_0)} |\Phi_I\rangle, \quad (1)$$

where E_I is the corresponding eigenenergy and the coefficient C_I determines the population distribution for each eigenstate. The coherent superposition has emerged at time t_0 due to crossing a conical intersection or the excitation by a pump pulse. We assume that an ultrashort XUV probe pulse interacts with the molecule at time t_p , which leads to an emission of a photoelectron. The momentum distribution of the photoelectron encodes information about the electronic state at the time t_p . In our study, we propose to probe electron dynamics by studying the momentum distribution of photoelectrons emitted from outermost orbitals that became populated due to the photoexcitation of the molecule. We use atomic units for this and following expressions.

Assuming a probe pulse with the central photon energy ω_{in} , polarization ϵ_{in} , pulse duration τ_p and intensity profile $I(t) = I_0 e^{-4 \ln 2 [(t-t_p)/\tau_p]^2}$, the general expression for the photoelectron probability is [7]

$$P(\mathbf{q}, t_p) = \frac{\tau_p^2 I_0 |\epsilon_{in} \cdot \mathbf{q}|^2}{8\pi \ln 2 \omega_{in}^2 c} \sum_{F,\sigma} e^{-(\Omega_F - \epsilon_e)^2 \tau_p^2 / (4 \ln 2)} \times \left| \chi_\sigma^\dagger \int d^3 r e^{-i\mathbf{q}\cdot\mathbf{r}} \phi_F^D(\mathbf{r}, t_p) \right|^2, \quad (2)$$

where \mathbf{q} is the momentum of the photoelectron with the corresponding energy $\epsilon_e = \frac{|\mathbf{q}|^2}{2}$ and χ_σ is the photoelectron spin state. The summation is over all possible final states of the molecule $\langle \Phi_F^{N_{el}-1} |$ that can be produced after the photoionization by the probe pulse, E_F is their corresponding eigenenergy. $\phi_F^D(\mathbf{r}, t_p) = \langle \Phi_F^{N_{el}-1} | \hat{\psi}(\mathbf{r}) | \Psi(t_p) \rangle$ is the Dyson orbital defined as the overlap between the N_{el} wavefunction of the initial state of the system and the $(N_{el} - 1)$ wavefunction of the final state, where $\hat{\psi}(\mathbf{r})$ is the electron annihilation field operator. $\Omega_F = \omega_{in} + \langle E \rangle - E_F$, where $\langle E \rangle$ is the mean energy of the eigenstates involved in the wave-packet in Eq. (1). Here, we assumed the sudden approximation, *i. e.* the molecular state after photoionization and the state of the photoelectron are decoupled, which is justified for high kinetic photoelectron energies [72]. It is also assumed that the probe-pulse duration is much shorter than the characteristic time scale of the electron dynamics. This means that the energy splittings of the eigenstates involved in the dynamics are much smaller than the bandwidth of the probe pulse and can be substituted by their mean energy. If this assumption fails, the eigenenergies must enter the expression explicitly and Eq. (2) gets slightly modified

$$P(\mathbf{q}, t_p) \propto \sum_{F,\sigma} \left| \sum_I e^{-(\omega_{in} + E_I - E_F - \epsilon_e)^2 \tau_p^2 / (8 \ln 2)} \times \chi_\sigma^\dagger \int d^3 r e^{-i\mathbf{q}\cdot\mathbf{r}} \phi_{FI}^D(\mathbf{r}, t_p) \right|^2, \quad (3)$$

where $\phi_{FI}^D(\mathbf{r}, t_p) = \langle \Phi_F^{N_{el}-1} | \hat{\psi}(\mathbf{r}) | C_I e^{-iE_I(t_p-t_0)} \rangle$. Time- and angle-resolved photoelectron probability for molecules with electron dynamics has also been previously theoretically studied [66, 73–75]. Eqs. (2) and (3) take a broad bandwidth of a probe pulse accurately into account, which was not the case in these studies.

It follows from the expression Eq. (2) that the momentum-resolved photoelectron probability encodes the Fourier transform of the Dyson orbital. If the molecule is in the ground state, the overlap integral between a singly ionized molecule and the molecule before the ionization is well approximated by the Hartree-Fock (HF) orbital, from which an electron was detached. Due to this connection, photoelectron momentum microscopy is used as an orbital imaging method [76–78].

When a molecule in an excited state is ionized by a probe pulse, the Dyson orbital cannot be approximated by a molecular orbital and the interpretation of

the Dyson orbital becomes more challenging. In order to carefully describe the excited state dynamics as well as accurately treat the Dyson orbital, we describe the excited states involved in the dynamics $|\Phi_I\rangle$ and the states of the ionized molecule $\Phi_F^{N_{\text{el}}-1}$ using the configuration interaction method. We express each excited state based on the configuration interaction approach limited to single excitations as

$$|\Phi_I\rangle = \sum_{i_1, a_1} \tilde{c}_{i_1}^{a_1}(I) \left| \phi_{i_1}^{a_1, S(I)} \right\rangle, \quad (4)$$

where $\left| \phi_{i_1}^{a_1, S(I)} \right\rangle$ denotes a configuration state function (CSF), where an electron of the HF ground state has been excited from the orbital i_1 to the orbital a_1 . Such a state has a hole in orbital i_1 and an electron in orbital a_1 , and $S(I)$ describes the total spin and the spin projection value. For the description of the final state, we use a similar approach, but add one additional hole in the configuration space. Thus, the final state is

$$\begin{aligned} \left\langle \Phi_F^{N_{\text{el}}-1} \right| = & \sum_{i_2, j_2, a_2} \tilde{c}_{i_2, j_2}^{a_2}(F) \left\langle \phi_{i_2, j_2}^{a_2, S(F)} \right| \\ & + \sum_{i_2} \tilde{c}_{i_2}(F) \left\langle \phi_{i_2}^{S(F)} \right|, \end{aligned} \quad (5)$$

where $\left\langle \phi_{i_2, j_2}^{a_2, S(F)} \right|$ describes a CSF which contains two holes in orbitals i_2 and j_2 and an electron in orbital a_2 . We denote an $N_{\text{el}} - 1$ -electron CSF with one hole among originally occupied orbitals of the molecule (HOMO, HOMO-1, ...) and no electrons in the originally unoccupied molecular orbitals (LUMO, LUMO+1, ...) as $\left\langle \phi_{i_2}^{S(F)} \right|$. In both cases, $S(F)$ describes the total spin and the spin projection value of the final state F . The coefficients $\tilde{c}_{i_2, j_2}^{a_2}(F)$ and $\tilde{c}_{i_2}(F)$ determine the contribution of a CSF to the final state. We perform calculations employing RASSCF method [79] and use the same active orbitals for the treatment of the states $|\Phi_I\rangle$ and $\left\langle \Phi_F^{N_{\text{el}}-1} \right|$. With these approximations, the overlap integrals between neutral and singly-ionized eigenstates of a molecule are given by a linear combination of the overlap integrals between N_{el} - and $(N_{\text{el}} - 1)$ -electron CSFs. Such an overlap integral provide either a zero or a molecule orbital, which is occupied in a N_{el} -electron CSF and unoccupied in a $(N_{\text{el}} - 1)$ -electron CSF. Thus, a Dyson orbital can be represented as a linear combination of molecular orbitals.

III. IMAGING PHOTO-INDUCED DYNAMICS IN PENTACENE

Based on the previous considerations, we present an example for imaging excited-state dynamics in aligned isolated pentacene molecules. The molecular alignment

can be achieved either for gas-phase molecules or molecular films adsorbed on substrates. We recently observed that photo-excited dynamics of pentacene molecules in a top pentacene layer of a bilayer pentacene films adsorbed on an Ag(110) surface behave similarly to the dynamics of an isolated pentacene [15]. These dynamics were probed using time-resolved photoelectron momentum microscopy on a time scale of several hundreds of femtoseconds. This experiment established conditions for time-resolved photoelectron microscopy at free-electron lasers, which makes it feasible to perform such experiments at much shorter timescales with brilliant and ultrashort light pulses from free-electron laser sources.

In our study, we assume that coherent electron dynamics in pentacene were excited by a pump pulse via an optical excitation from the ground state. Since direct optical transitions from the ground state to triplet excited states are dipole forbidden, we truncate our considerations to spin-singlet excited states.

We calculate the vertical excited spin-singlet states of pentacene with MOLCAS [80] using the RASSCF method [79], with a CC-PVDZ basis set for the atoms [81, 82]. The calculation of the first excited states of pentacene is converged with an active space of 22 orbitals, containing 11π and $11\pi^*$ orbitals. Including more orbitals in the active space does not lead to significant changes in the energy spectrum and the structure of the eigenstates. The π orbitals contain a maximum of one hole, while the π^* orbitals have a maximum of one electron. The energies of the first four excited states and the changes in the occupation of the orbitals (compared to the HF ground state) are shown in Fig. 1. We find that the third and the fourth excited singlet states are dark states and the next bright singlet states are energetically highly separated from the first and the second excited state. Thus, one would be able to create a coherent superposition of just two excited states of a pentacene in a possible experiment. When the coherent superposition of the two excited states of pentacene is created, its electron density starts to oscillate in time. The oscillation period is determined by the energy difference between the excited states. The energy difference and the electronic wavefunctions of the bright excited states obtained in our calculation agree well with the experimental and theoretical results in previous studies [83–85]. Also, the agreement with a more accurate CASPT2 calculation [85] justifies our chosen theoretical level of single excitation in the configuration space. We obtain that the first excited state is predominantly characterized by the CSF obtained by the excitation of an electron from the HOMO to the LUMO. The second excited state is predominantly characterized by a linear combination of the CSF obtained by the excitation of an electron from the HOMO to the LUMO+2 and the CSF obtained by the excitation of an electron from the HOMO-2 to the LUMO.

The energy difference between the two excited states results in an oscillation period of the electron density of $T = 5.73$ fs. To simplify our considerations, we can ne-

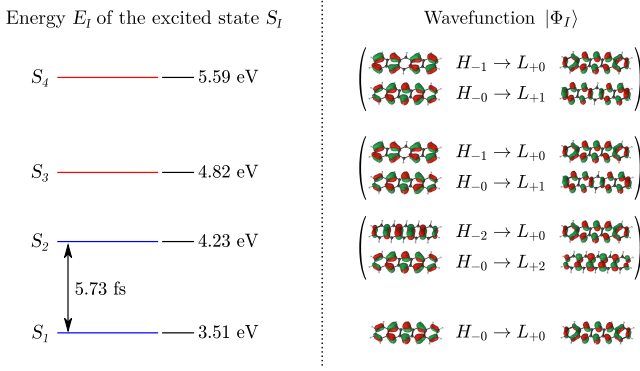


FIG. 1. Energy level diagram of the first four vertical spin-singlet excited states of pentacene (left), with bright states in blue and dark states in red. A wave-packet in a coherent superposition of the first two excited states has an oscillation period of 5.73 fs. The corresponding orbital excitations contribute to the wave function of the states (right), while the arrow means an excitation from the left (HOMO- i) to the right (LUMO+ j) orbital. For the visualization of the orbitals, we used the software LUSCUS [86]

glect nuclear motions that should affect electron dynamics on longer time scales. With Eq. (1) the time evolution of the wave-packet after the excitation by the pump pulse at $t_0 = 0$ is

$$|\Psi(t)\rangle = C_1 e^{-iE_1 t} |\Phi_1\rangle + C_2 e^{-iE_2 t} |\Phi_2\rangle, \quad (6)$$

$$|\Phi_1\rangle = \left| \phi_H^{L,0(0)} \right\rangle, \quad (7)$$

$$|\Phi_2\rangle = \frac{1}{\sqrt{2}} \left(\left| \phi_H^{L+2,0(0)} \right\rangle - \left| \phi_{H-2}^{L,0(0)} \right\rangle \right), \quad (8)$$

with $|C_1|^2 + |C_2|^2 = 1$. The coefficients C_1 and C_2 depend on a particular process, which brought a molecule into a coherent superposition of electronic states. Our results do not depend on the particular values of the coefficients C_1 and C_2 and we assume an equal population of both excited states, $C_1 = C_2 = \frac{1}{\sqrt{2}}$. The orbital index $H - i$ denotes the i -th orbital below the HOMO and $L + j$ is the j -th orbital above the LUMO. The photo-excitation leads to a time-dependent change in the electron density relative to the ground state density

$$\rho_{ex}(\mathbf{r}, t) = \rho_1(\mathbf{r}, t) - \rho_0(\mathbf{r}), \quad (9)$$

where $\rho_0(\mathbf{r}) = \langle \Phi_0 | \hat{\psi}^\dagger(\mathbf{r}) \hat{\psi}(\mathbf{r}) | \Phi_0 \rangle$ is the electron density of the ground state of pentacene described by the wave function $|\Phi_0\rangle$. The electron density for the pentacene after the photo-excitation by a pump pulse is $\rho_1(\mathbf{r}, t) = \langle \Psi(t) | \hat{\psi}^\dagger(\mathbf{r}) \hat{\psi}(\mathbf{r}) | \Psi(t) \rangle$. We evaluate the electron density

change and obtain

$$\begin{aligned} \rho_{ex}(\mathbf{r}, t) = & \left| C_1^* e^{iE_1 t} \phi_L(\mathbf{r}) + \frac{C_2^*}{\sqrt{2}} e^{iE_2 t} \phi_{L+2}(\mathbf{r}) \right|^2 \\ & + \frac{|C_2|^2}{2} |\phi_L(\mathbf{r})|^2 - \frac{|C_2|^2}{2} |\phi_H(\mathbf{r})|^2 \\ & - \left| C_1^* e^{iE_1 t} \phi_H(\mathbf{r}) - \frac{C_2^*}{\sqrt{2}} e^{iE_2 t} \phi_{H-2}(\mathbf{r}) \right|^2, \end{aligned} \quad (10)$$

where $\phi_{H-i}(\mathbf{r})$ and $\phi_{L+j}(\mathbf{r})$ are the wavefunctions of the i -th orbital below the HOMO and the j -th orbital above the LUMO. The electron density change is shown in Fig. 2 at different times during the oscillation period. The negative (blue) part is the reduction of the electron density compared to the ground state density and the positive (yellow) part is the increase of the electron density compared to the ground state density. The time-dependent part of the electron density oscillates in time as $\cos[(E_1 - E_2)t]$. From $t = 0$ to $t = \frac{T}{2}$, the photo-induced negative charge flows from the top left and bottom right of the molecule to the top right and bottom left. The photo-induced positive charge flows in the opposite direction. The spatial distribution of the electron density change at $t = \frac{T}{2}$ can be mapped onto the electron density change at $t = 0$ by a reflection in the yz -plane. At two times during the oscillation period, $t = \frac{T}{4}$ and $t = \frac{3T}{4}$, the photo-excited change in the electron density coincides and has reflection symmetry.

We assume that an XUV probe pulse with the central energy of 100 eV and 500 as duration photoionizes the molecule at the pump-probe time delay t_p . The probe pulse is linearly polarized along the y -direction, which is perpendicular to the nodal plane of the molecule. For the calculation of the final states after the photoionization by the probe pulse, we apply the same method as in the calculation of the excited states of pentacene, but with an additional hole in the 11 active π orbitals. Tab. I shows the first six final states of pentacene with the lowest energy that can be reached by ionizing the initial state in Eq. (6).

If the photoionization was triggered by a pulse with a narrow bandwidth, the photoelectron probability as a function of energy would consist of clear spectral lines centred at energies $\Omega_{F,I} = E_F - E_I - \omega_{in} + \epsilon_e$. Thus, the photoelectron momentum distributions would be clearly assigned to a certain Dyson orbital. In the case of the ultrashort probe pulse, each spectral line has the spectral band width of 5.16 eV and an individual Dyson orbital contributing to the momentum distribution at a given energy is no longer distinguished.

Let us first consider the angle-integrated photoelectron spectra. In a real experiment, a probe pulse would interact with a number of pentacene molecules, some of which would be excited by a pump pulse, and some of which would remain unexcited. Thus, we first estimate, how the photoionization from unexcited pentacene molecules would affect the photoelectron spectra from pentacene

F	E_F	Ω_F	$\langle \Phi_F^{N_{el}-1} $
1	5.0 eV	98.9 eV	$-0.95 \langle \Phi_H^{1/2(1/2)} $
2	6.7 eV	97.2 eV	$-0.94 \langle \Phi_{H-2}^{1/2(1/2)} $
3	7.5 eV	96.4 eV	$-0.83 \langle \Phi_{H,H}^{L,1/2(1/2)} + 0.31 \langle \Phi_{H-4}^{1/2(1/2)} $
4	8.7 eV	95.2 eV	$-0.62 \langle \Phi_{H,H}^{L+1,1/2(1/2)} + 0.5 \langle \Phi_{H-1,H}^{L,1/2(1/2)} _{udu} + 0.28 \langle \Phi_{H-1,H}^{L,1/2(1/2)} _{uud}$
5	9.6 eV	94.3 eV	$0.70 \langle \Phi_{H-1,H}^{L,1/2(1/2)} _{uud} - 0.45 \langle \Phi_{H-1,H}^{L,1/2(1/2)} _{udu}$
6	9.7 eV	94.2 eV	$-0.59 \langle \Phi_{H,H}^{L+2,1/2(1/2)} + 0.62 \langle \Phi_{H-2,H}^{L,1/2(1/2)} _{udu} - 0.28 \langle \Phi_{H-2,H}^{L,1/2(1/2)} _{uud}$

TABLE I. First six final states $|\Phi_F\rangle$ of ionized and excited pentacene, which result in a nonzero Dyson orbital $\phi_F^D(\mathbf{r}) = \langle \Phi_F^{N_{el}-1} | \hat{\psi}(\mathbf{r}) | \Psi(t) \rangle$. The corresponding energy is E_F and $\Omega_F = E_F - \langle E \rangle - \omega_{in} + \epsilon_e$ is the central energy in the photoelectron probability in Eq. (2) for the given final state. The right column shows the contributing configuration state functions of the final state. The indices *udu* and *uud* distinguish two different CSFs that result in the total spin of 1/2 and spin projection of +1/2.

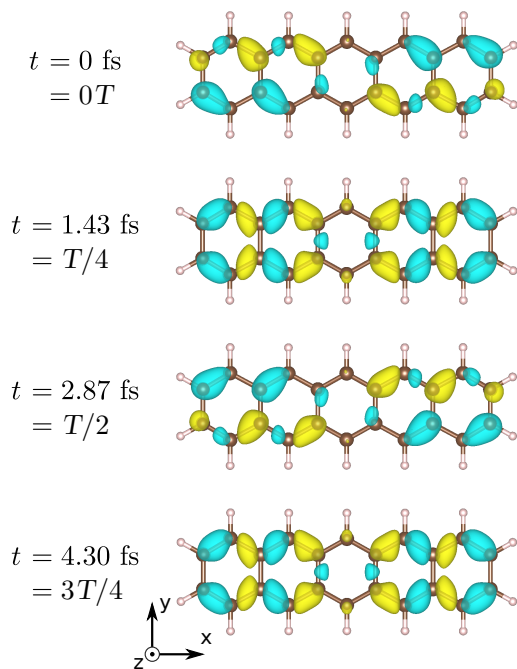


FIG. 2. The time evolution of the electron-hole density after the excitation of the pentacene molecule to the first two excited states with the pump pulse at $t_0 = 0$ fs. The blue isosurface shows the hole density (negative value) and the yellow the electron density (positive value). For the visualization we used the software VESTA [87].

molecules in the excited state. In Fig. 3, we show photoelectron spectra from the pentacene molecules being in the ground state S_0 and from pentacene molecules being in the coherent superposition of the excited state S_1 and S_2 ($|\Psi(t)\rangle$ in Eq. (6)). We obtain that the contribution

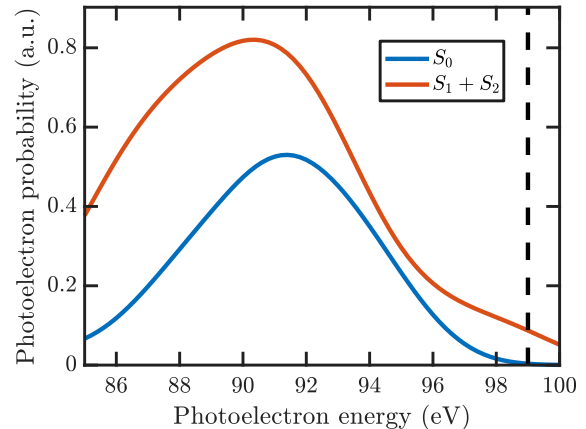


FIG. 3. Angle-integrated photoelectron spectra for photoelectrons detached either from the ground state S_0 or in the coherent superposition of the excited state S_1 and S_2 . The black dotted line shows the contribution at the photoelectron energy $\epsilon_e = 99$ eV. The probe-pulse duration is 0.5 fs and has a central photon energy of 100 eV.

of photoelectrons detached from unexcited molecules is negligible at energies higher than 97 eV. Thus, photoelectron spectra at energies higher than 97 eV are beneficial to study the dynamics of photoexcited pentacene molecules, since they would not contain a background signal from the unexcited molecules.

We find a remarkable result that the angle-averaged photoelectron spectra from photo-excited pentacene do not vary with the probe-pulse arrival time although the photo-induced charge distribution experiences considerable oscillations in time (see Fig. 2). This is because the time-dependent part of the electronic density change is highly symmetric in space. As a consequence, the photoelectron momentum distributions are also highly

symmetric and the temporal dependence of the signal averages out after the angle integration. The angle-integrated spectra do not reveal information about the time-dependent photo-induced charge oscillations.

We now demonstrate that photoelectron momentum microscopy is indeed quite sensitive to photo-induced electron dynamics. We consider photoelectron momentum maps (PMMs) of a photoelectron with a fixed kinetic energy of $\epsilon_e = 99$ eV. PMMs are constructed by a two-dimensional projection of the three-dimensional photoelectron momentum distribution for a constant energy ϵ_e (hemispherical cuts). Based on Eq. (2), the photoelectron probability resulting from a particular final state is only time-dependent, if the final state has a nonzero overlap with both eigenstates in the initial state, $\langle \Phi_F | \hat{\psi}(\mathbf{r}) | \Phi_1 \rangle \neq 0$ and $\langle \Phi_F | \hat{\psi}(\mathbf{r}) | \Phi_2 \rangle \neq 0$. At the chosen kinetic energy, three final states with the lowest energies, with the indices 1, 2 and 3 in Table I contribute to the PMM. Thereby, among these three final states, only the final state 1 contributes to a time-dependent signal and the other two final states 2 and 3 contribute to a time-independent background. The first final state results in a

broad spectral line centered approximately at the energy $\epsilon_e = 99$ eV.

We derive the explicit expressions for the Dyson orbital that determine the angle-resolved photoelectron spectra at $\epsilon_e = 99$ eV. For the first three final states, we obtain

$$\begin{aligned} \phi_{F_1}^D(\mathbf{r}) &= \langle \Phi_{F_1} | \hat{\psi}(\mathbf{r}) | \Psi(t) \rangle \\ &= -C_1 e^{-iE_1 t_p} \frac{0.95}{\sqrt{2}} \phi_L(\mathbf{r}) \chi_{\downarrow} \\ &\quad - C_2 e^{-iE_2 t_p} \frac{0.95}{2} \phi_{L+2}(\mathbf{r}) \chi_{\downarrow}, \end{aligned} \quad (11)$$

$$\begin{aligned} \phi_{F_2}^D(\mathbf{r}) &= \langle \Phi_{F_2} | \hat{\psi}(\mathbf{r}) | \Psi(t) \rangle \\ &= C_2 e^{-iE_2 t_p} \frac{0.94}{2} \phi_L(\mathbf{r}) \chi_{\downarrow}, \end{aligned} \quad (12)$$

$$\begin{aligned} \phi_{F_3}^D(\mathbf{r}) &= \langle \Phi_{F_3} | \hat{\psi}(\mathbf{r}) | \Psi(t) \rangle \\ &= -C_1 e^{-iE_1 t_p} \frac{0.83}{\sqrt{2}} \phi_H(\mathbf{r}) \chi_{\downarrow}. \end{aligned} \quad (13)$$

These three Dyson orbitals in Eqs. (11) - (13) enter the photoelectron probability in Eq. (2) at the photoelectron energy $\epsilon = 99$ eV

$$\begin{aligned} P(\mathbf{q}, t_p) &\underset{\epsilon_e=99 \text{ eV}}{\propto} |\boldsymbol{\epsilon}_{\text{in}} \cdot \mathbf{q}|^2 \left[e^{-(\Omega_{F_1} - \epsilon_e)^2 \frac{\tau_p^2}{4 \ln^2}} \left| C_1 e^{-iE_1 t_p} \frac{0.95}{\sqrt{2}} \mathcal{F}(\phi_L(\mathbf{r}))(\mathbf{q}) + C_2 e^{-iE_2 t_p} \frac{0.95}{2} \mathcal{F}(\phi_{L+2}(\mathbf{r}))(\mathbf{q}) \right|^2 \right] \\ &\quad + |\boldsymbol{\epsilon}_{\text{in}} \cdot \mathbf{q}|^2 \left[e^{-(\Omega_{F_2} - \epsilon_e)^2 \frac{\tau_p^2}{4 \ln^2}} \left| C_2 \frac{0.94}{2} \mathcal{F}(\phi_L(\mathbf{r}))(\mathbf{q}) \right|^2 + e^{-(\Omega_{F_3} - \epsilon_e)^2 \frac{\tau_p^2}{4 \ln^2}} \left| C_1 \frac{0.83}{\sqrt{2}} \mathcal{F}(\phi_H(\mathbf{r}))(\mathbf{q}) \right|^2 \right], \end{aligned} \quad (14)$$

where $\mathcal{F}(\phi(\mathbf{r}))(\mathbf{q}) = (2\pi)^{-3/2} \int d\mathbf{r}^3 e^{i\mathbf{q} \cdot \mathbf{r}} \phi(\mathbf{r})$ denotes the Fourier transform of an orbital $\phi(\mathbf{r})$. The resulting time-resolved PMMs shown in Fig. 4 vary strongly with time. The PMMs at $t_p = 0$ and $t_p = \frac{T}{2}$ are the point reflection image of each other and have the same symmetry as the changes of the electron density at these times (see Fig. 2). The PMMs at $t_p = \frac{T}{4}$ and $t_p = \frac{3T}{4}$, when the electron density coincides, are equal and have reflection symmetry. The most pronounced oscillating peaks are located in the PMMs at the momenta $q_x = \pm 1.26 \text{ \AA}^{-1}$ and $q_y = \pm 1.97 \text{ \AA}^{-1}$. According to Eq. (14) the time-dependent part of the PMMs arises from the Fourier transform of LUMO and LUMO+2 orbitals. It is directly related to the negatively-charged part of the induced electron-density change (yellow in Fig. 2), which is also specified by the LUMO and LUMO+2 orbitals (see Eq. (10)). Thus, the time-dependent features in the PMMs encode the information about the symmetry of the photo-induced electron density. Due to a high contrast of a signal and a low background, these features can be detected in an experiment even if the signal is weak. Due to the high spatial resolution, PMMs resolve oscillations of the electron density within the molecule.

In Ref. [7, 88], we demonstrated that that a general time- and momentum-resolved signal from a coherently evolving electronic wave packet can be sensitive to electron currents within a sample. This means that a momentum-resolved signal can be even different, when the electron density coincides, but the charge flow direction differs. This applies to the electronic state in Fig. 2 at times $t_p = \frac{T}{4}$ and $t_p = \frac{3T}{4}$. However, we do not observe this effect in the considered case, since it also averages out due to the high symmetry of the photo-induced charge distribution.

Finally, we investigate PMMs and their temporal dependence at different photoelectron energies in Fig. 5. As follows from the angle-integrated spectra in Fig. 3, the overall intensity of the PMMs increases at lower photoelectron energies. The PMMs at energy $\epsilon_e = 90$ eV and at energy $\epsilon_e = 96$ eV remain almost constant in time, whereas the PMMs at $\epsilon_e = 93$ eV and at $\epsilon_e = 99$ eV show pronounced temporal dependence. Although the absolute change of the signal in time is approximately the same in the two former cases, the overall contrast is much better for the PMMs at $\epsilon_e = 99$ eV due to a lower time-constant background. This temporal behavior of the signal can be explained by the character of photo-

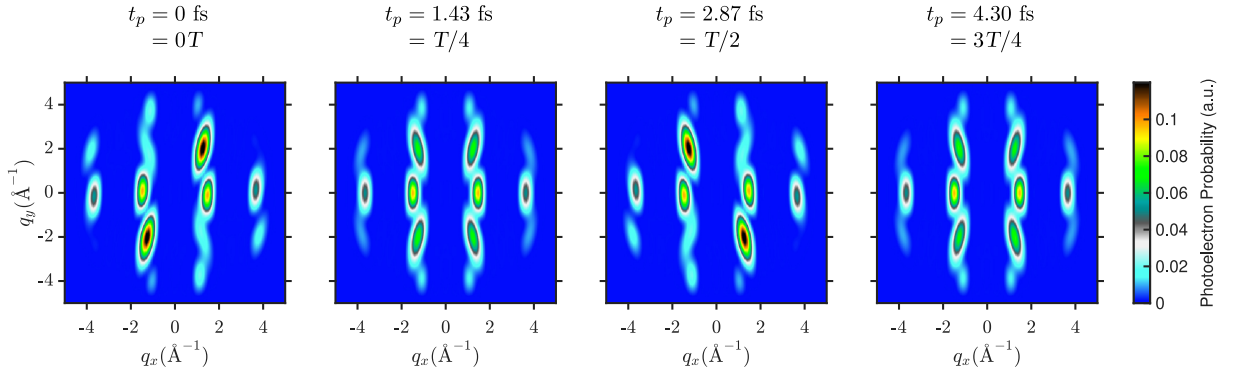


FIG. 4. Time-dependent photoelectron momentum maps for photoelectrons emitted from the excited pentacene at different probe-pulse arrival times t_p . The probe-pulse duration is 0.5 fs and the central photon energy is 100 eV. The momentum maps are shown at the photoelectron energy of $\epsilon_e = 99$ eV.

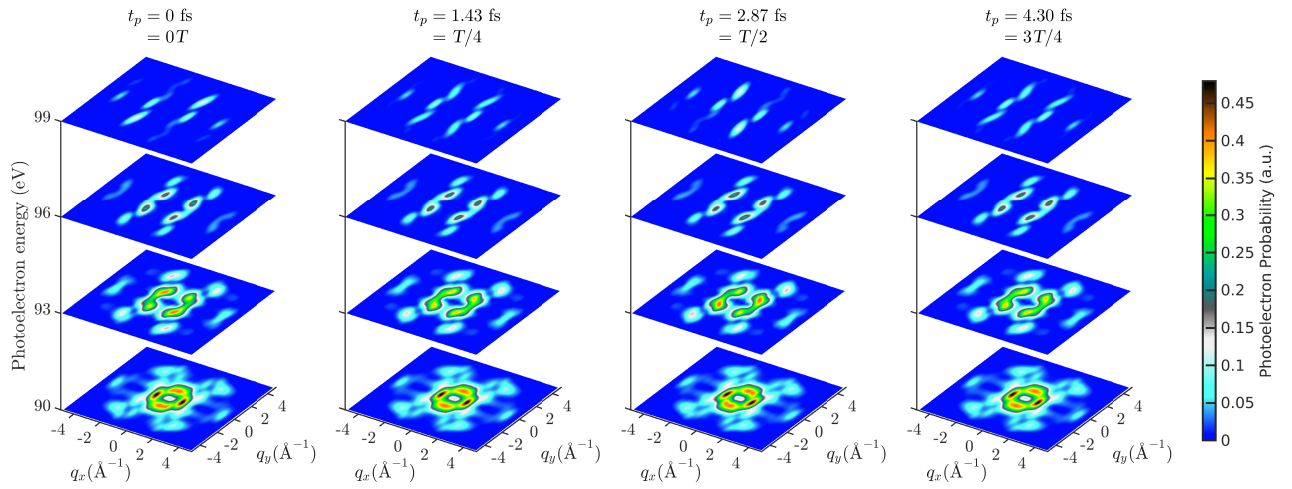


FIG. 5. Time-dependent photoelectron momentum maps for photoelectrons emitted from the excited pentacene for different photoelectron energies ϵ_e . Each set of momentum maps has a different probe-pulse arrival time t_p . The probe-pulse duration is 0.5 fs and the central photon energy is 100 eV.

induced changes in the electron density. These changes are due to the electrons photo-excited into orbitals that were unoccupied in the ground state and holes in the orbitals that were doubly occupied in the ground state. If an electron, which evolves in the photo-excited orbitals, is emitted by a probe pulse, then it directly carries the information about the negatively-charged oscillations of the electron density. If an electron is indeed emitted from lower lying orbitals, where an electron hole evolves, then it is an "indirect probe" of the evolving hole. Thus, the signal at the photoelectron energy of 99 eV results from the emission of electrons evolving in the photo-excited orbitals and is the most advantageous to obtain a time-resolved signal with a high contrast.

In a real experiment, PMMs would be obtained with limited energy and time resolution. We simulate the PMMs in the case of limited energy resolution by averaging the photoelectron probability over the corresponding energy interval. We show the PMMs at the photoelec-

tron energy of 99 eV assuming the energy resolution of 1 eV in Figs. 6(a)-(d), which are obtained by averaging the signal over the range of 98.5 eV to 99.5 eV. We obtain that the momentum distributions are almost unaffected by the limited energy resolution.

The temporal resolution of the experiment is determined by the duration of the probe pulse and the timing jitter between the probe and the pump pulses. If the probe-pulse duration cannot be assumed to be much shorter than the oscillation period, Eq. (3) must be used for the calculation instead of Eq. (2). We calculate the signal with Eq. (3) at different probe-pulse durations τ_p . We also assume the limited energy resolution of 1 eV. As shown in Figs. 6(e)-(h) and Figs. 6(i)-(l), the temporal contrast of the resulting signal is quite high even, if the probe-pulse duration is as large as a quarter or half of the oscillation period.

In our calculation, we neglected electron-nuclear coupling in the description of charge migration since the

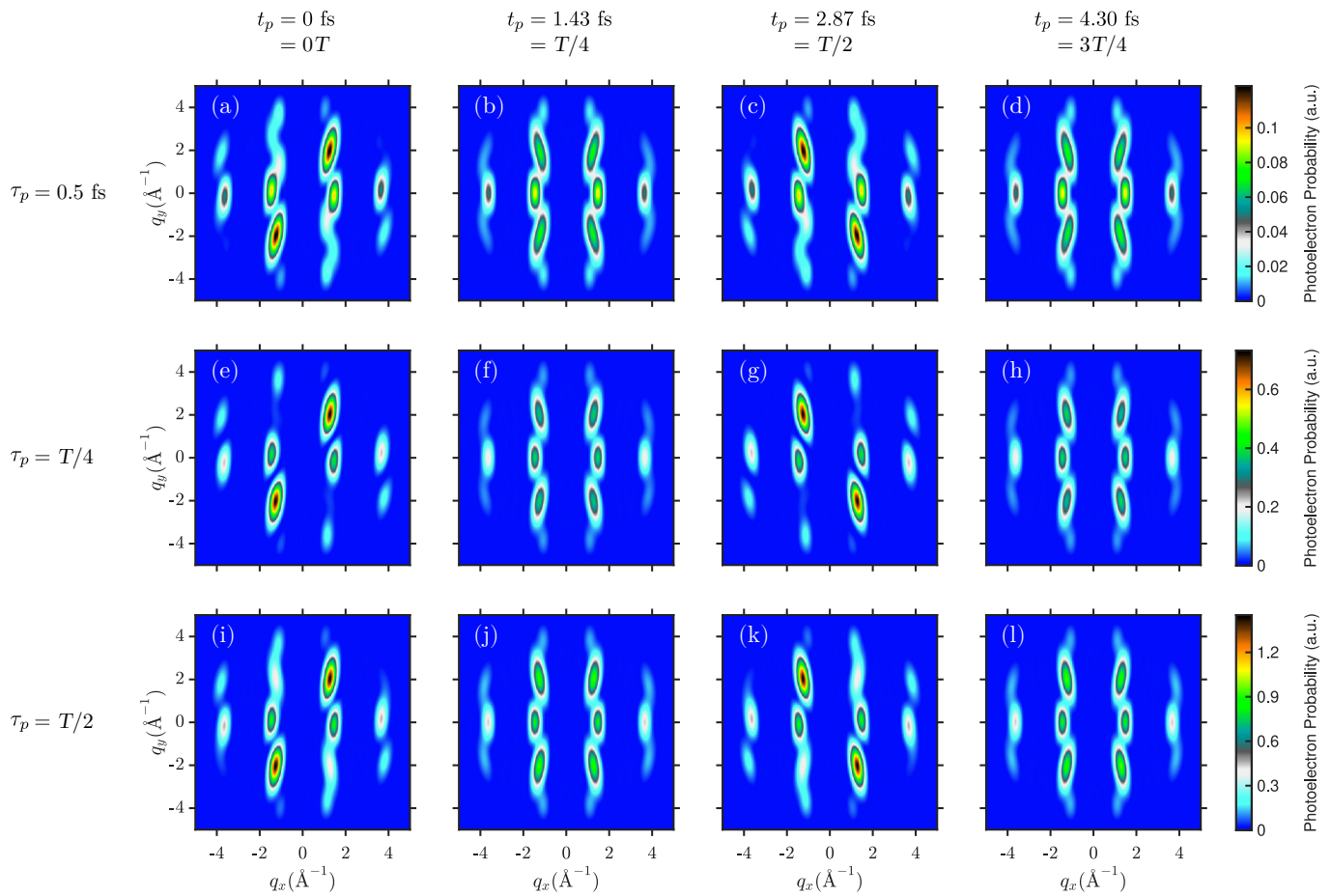


FIG. 6. Time-dependent photoelectron momentum maps (PMMs) for photoelectrons emitted from the excited pentacene. In each column the PMMs are shown for different probe-pulse arrival times (a),(e),(i) $t_p = 0T$, (b),(f),(j) $t_p = T/4$, (c),(g),(k) $t_p = T/2$, (d),(h),(l) $t_p = 3T/4$. In the different rows the PMMs are shown for different probe-pulse durations (a)-(d) $\tau_p = 0.5$ fs, (e)-(h) $\tau_p = T/4$, (i)-(l) $\tau_p = T/2$. The probe pulse has a central photon energy of 100 eV. The momentum maps are obtained by averaging the signal over the range of $\epsilon_e = 98.5$ eV to $\epsilon_e = 99.5$ eV to simulate the energy resolution of 1 eV.

primary goal of our study is to investigate how pure electron dynamics on their natural time scale can be measured. Let us discuss, which consequences the coupling of electron dynamics to nuclear dynamics would have for the signal. The coupling to nuclear motions would indeed lead to decoherence of electron dynamics and should cause the decrease of the oscillation amplitude [41, 65, 89, 90]. Former studies of coupled electron-nuclear dynamics of similar molecules such as norbornadiene cations [91] or benzene [92] have demonstrated that coherent electron motion can last up to 20 fs in these molecules. It is expected that coherent electronic motion in polycyclic aromatic hydrocarbons, which also include pentacene, would experience similar time scales [92]. Since 20 fs corresponds to about five cycles of oscillation in our case, our assumption that charge migration is coherent during at least one full oscillation period is robust. At longer time scales, the decay of the amplitude of the periodic charge oscillations due to decoherence would result in the decrease of the time-dependent changes in the PMMs. This would lead to a loss of tem-

poral contrast of the signal, which means that the signal at different times would become less distinguishable from the time-independent part of the signal (see Fig. 5). This could serve even as an advantage, since such an experiment would reveal the transition of coherent dynamics to decoherent dynamics.

IV. CONCLUSIONS

We showed theoretically how time-resolved photoelectron momentum microscopy can be employed to image photo-induced coherently evolving electron dynamics in a pentacene molecule. The assumed XUV probe pulse of 500 as duration provides the temporal resolution, which is sensitive to pure intramolecular electronic dynamics. The momentum-resolved signal revealed details of electron dynamics with Ångstrom spatial resolution. Although the angle-averaged photoelectron spectra were not sensitive to electron dynamics, momentum-resolved spectra provided a highly contrast signal evolving in time.

At high photoelectron energies, the signal is provided by the electrons emitted from photo-excited orbitals and is not affected from a possible contribution of photoelectrons emitted by molecules that were not photo-excited. Such photoelectron momentum maps are directly related to the negatively-charged part of the photo-induced changes in the electron density and is sensitive to its symmetry in real space. These findings demonstrate that attosecond photoelectron momentum microscopy has a big potential to become a novel technique to measure

charge migration and electron coherence processes in exciton transport in organic semiconductors with unprecedented time and spatial details.

V. ACKNOWLEDGEMENTS

We gratefully acknowledge the funding of the Volkswagen Foundation.

-
- [1] Christer Z. Bisgaard, Owen J. Clarkin, Guorong Wu, Anthony M. D. Lee, Oliver Geßner, Carl C. Hayden, and Albert Stolow. Time-resolved molecular frame dynamics of fixed-in-space CS₂ molecules. *Science*, 323(5920):1464–1468, 2009.
- [2] Peter Puschnig, Stephen Berkebile, Alexander J. Fleming, Georg Koller, Konstantin Emtsev, Thomas Seyller, John D. Riley, Claudia Ambrosch-Draxl, Falko P. Netzer, and Michael G. Ramsey. Reconstruction of molecular orbital densities from photoemission data. *Science*, 326(5953):702–706, 2009.
- [3] Daniel Lüftner, Thomas Ules, Eva Maria Reinisch, Georg Koller, Serguei Soubatch, F. Stefan Tautz, Michael G. Ramsey, and Peter Puschnig. Imaging the wave functions of adsorbed molecules. *Proceedings of the National Academy of Sciences*, 111(2):605–610, 2014.
- [4] B. Mignolet, R. D. Levine, and F. Remacle. Control of electronic dynamics visualized by angularly resolved photoelectron spectra: A dynamical simulation with an ir pump and xuv attosecond-pulse-train probe. *Phys. Rev. A*, 89:021403, Feb 2014.
- [5] Peter Puschnig and Daniel Lüftner. Simulation of angle-resolved photoemission spectra by approximating the final state by a plane wave: From graphene to polycyclic aromatic hydrocarbon molecules. *Journal of Electron Spectroscopy and Related Phenomena*, 200(xx):193–208, 2015.
- [6] S. Weiß, D. Lüftner, T. Ules, E. M. Reinisch, H. Kaser, A. Gottwald, M. Richter, S. Soubatch, G. Koller, M. G. Ramsey, F. S. Tautz, and P. Puschnig. Exploring three-dimensional orbital imaging with energy-dependent photoemission tomography. *Nature Communications*, 6:8287, October 2015.
- [7] Daria Popova-Gorelova, Jochen Küpper, and Robin Santra. Imaging electron dynamics with time- and angle-resolved photoelectron spectroscopy. *Phys. Rev. A*, 94:013412, Jul 2016.
- [8] P Kliuiev, T Latychevskaja, J Osterwalder, M Hengsberger, and L Castiglioni. Application of iterative phase-retrieval algorithms to ARPES orbital tomography. *New Journal of Physics*, 18(9):093041, sep 2016.
- [9] C. W. Nicholson, A. Lücke, W. G. Schmidt, M. Puppin, L. Rettig, R. Ernstorfer, and M. Wolf. Beyond the molecular movie: Dynamics of bands and bonds during a photoinduced phase transition. *Science*, 362(6416):821–825, 2018.
- [10] Pavel Kliuiev, Giovanni Zamborlini, Matteo Jugovac, Yeliz Gurdal, Karin von Arx, Kay Waltar, Stephan Schnidrig, Roger Alberto, Marcella Iannuzzi, Vitaliy Feyer, Matthias Hengsberger, Jürg Osterwalder, and Luca Castiglioni. Combined orbital tomography study of multi-configurational molecular adsorbate systems. *Nature Communications*, 10(1):5255, Nov 2019.
- [11] C. Metzger, M. Graus, M. Grimm, G. Zamborlini, V. Feyer, M. Schwendt, D. Lüftner, P. Puschnig, A. Schöll, and F. Reinert. Plane-wave final state for photoemission from nonplanar molecules at a metal-organic interface. *Physical Review B*, 101(16):165421, April 2020. Publisher: American Physical Society.
- [12] G S M Jansen, M Keunecke, M Düvel, C Möller, D Schmitt, W Bennecke, F J S Kappert, D Steil, D R Luke, S Steil, and S Mathias. Efficient orbital imaging based on ultrafast momentum microscopy and sparsity-driven phase retrieval. *New Journal of Physics*, 22(6):063012, jun 2020.
- [13] R. Wallauer, M. Raths, K. Stallberg, L. Münster, D. Brandstetter, X. Yang, J. Güdde, P. Puschnig, S. Soubatch, C. Kumpf, F. C. Bocquet, F. S. Tautz, and U. Höfer. Tracing orbital images on ultrafast time scales. *Science*, 371(6533):1056–1059, 2021.
- [14] Alexander Neef, Samuel Beaulieu, Sebastian Hammer, Shuo Dong, Julian Maklar, Tommaso Pincelli, R. Patrick Xian, Martin Wolf, Laurenz Rettig, Jens Pflaum, and Ralph Ernstorfer. Orbital-resolved observation of singlet fission, 2022.
- [15] Kiana Baumgärtner, Marvin Reuner, Christian Metzger, Dmytro Kutnyakhov, Michael Heber, Federico Pressacco, Chul-Hee Min, Thiago RF Peixoto, Mario Reiser, Chan Kim, et al. Ultrafast orbital tomography of a pentacene film using time-resolved momentum microscopy at a fel. *Nature Communications*, 13(1):1–7, 2022.
- [16] N. Hartmann, G. Hartmann, R. Heider, M. S. Wagner, M. Ilchen, J. Buck, A. O. Lindahl, C. Benko, J. Grünert, J. Krzywinski, J. Liu, A. A. Lutman, A. Marinelli, T. Maxwell, A. A. Miahnahri, S. P. Moeller, M. Planas, J. Robinson, A. K. Kazansky, N. M. Kabachnik, J. Viehhaus, T. Feurer, R. Kienberger, R. N. Coffee, and W. Helml. Attosecond time-energy structure of x-ray free-electron laser pulses. *Nature Photonics*, 12(4):215–220, Apr 2018.
- [17] Praveen Kumar Maroju, Cesare Grazioli, Michele Di Fraia, Matteo Moioli, Dominik Ertel, Hamed Ahmadi, Oksana Plekan, Paola Finetti, Enrico Allaria, Luca Giannessi, Giovanni De Ninno, Carlo Spezzani, Giuseppe Penco, Simone Spampinati, Alexander Demidovich, Miltcho B. Danailov, Roberto Borghes, George Kourousias, Carlos Eduardo Sanches Dos Reis, Fulvio Billé, Alberto A. Lutman, Richard J. Squibb,

- Raimund Feifel, Paolo Carpeggiani, Maurizio Reduzzi, Tommaso Mazza, Michael Meyer, Samuel Bengtsson, Neven Ibrakovic, Emma Rose Simpson, Johan Mauritsson, Tamás Csizmadia, Mathieu Dumergue, Sergei Kühn, Harshitha Nandiga Gopalakrishna, Daehyun You, Kiyoshi Ueda, Marie Labeye, Jens Egebjerg Bækhoj, Kenneth J. Schafer, Elena V. Gryzlova, Alexei N. Grum-Grzhimailo, Kevin C. Prince, Carlo Callegari, and Giuseppe Sansone. Attosecond pulse shaping using a seeded free-electron laser. *Nature*, 578(7795):386–391, Feb 2020.
- [18] Joseph Duris, Siqi Li, Taran Driver, Elio G Champenois, James P MacArthur, Alberto A Lutman, Zhen Zhang, Philipp Rosenberger, Jeff W Aldrich, Ryan Coffee, et al. Tunable isolated attosecond x-ray pulses with gigawatt peak power from a free-electron laser. *Nature Photonics*, 14(1):30–36, 2020.
- [19] S. M. Teichmann, F. Silva, S. L. Cousin, M. Hemmer, and J. Biegert. 0.5-keV soft x-ray attosecond continua. *Nature Communications*, 7(1):11493, May 2016.
- [20] Jie Li, Xiaoming Ren, Yanchun Yin, Kun Zhao, Andrew Chew, Yan Cheng, Eric Cunningham, Yang Wang, Shuyuan Hu, Yi Wu, Michael Chini, and Zenghu Chang. 53-attosecond x-ray pulses reach the carbon k-edge. *Nature Communications*, 8(1):186, Aug 2017.
- [21] Xiaoming Ren, Jie Li, Yanchun Yin, Kun Zhao, Andrew Chew, Yang Wang, Shuyuan Hu, Yan Cheng, Eric Cunningham, Yi Wu, Michael Chini, and Zenghu Chang. Attosecond light sources in the water window. *Journal of Optics*, 20(2):023001, Jan 2018.
- [22] Jie Li, Jian Lu, Andrew Chew, Seunghwoi Han, Jialin Li, Yi Wu, He Wang, Shambhu Ghimire, and Zenghu Chang. Attosecond science based on high harmonic generation from gases and solids. *Nature Communications*, 11(1):2748, Jun 2020.
- [23] Giulio Maria Rossi, Roland E. Mainz, Yudong Yang, Fabian Scheiba, Miguel A. Silva-Toledo, Shih-Hsuan Chia, Phillip D. Keathley, Shaobo Fang, Oliver D. Mücke, Cristian Manzoni, Giulio Cerullo, Giovanni Cirmi, and Franz X. Kärtner. Sub-cycle millijoule-level parametric waveform synthesizer for attosecond science. *Nature Photonics*, 14(10):629–635, Oct 2020.
- [24] Bárbara Buades, Antonio Picón, Emma Berger, Iker León, Nicola Di Palo, Seth L. Cousin, Caterina Cocchi, Eric Pellegrin, Javier Herrero Martin, Samuel Mañas-Valero, Eugenio Coronado, Thomas Danz, Claudia Draxl, Mitsuharu Uemoto, Kazuhiro Yabana, Martin Schultze, Simon Wall, Michael Zürch, and Jens Biegert. Attosecond state-resolved carrier motion in quantum materials probed by soft x-ray xanes. *Applied Physics Reviews*, 8(1):011408, 2021.
- [25] Katsumi Midorikawa. Progress on table-top isolated attosecond light sources. *Nature Photonics*, 16(4):267–278, Apr 2022.
- [26] F. Calegari, D. Ayuso, A. Trabattoni, L. Belshaw, S. De Camillis, S. Anumula, F. Frassetto, L. Poletto, A. Palacios, P. Declava, J. B. Greenwood, F. Martín, and M. Nisoli. Ultrafast electron dynamics in phenylalanine initiated by attosecond pulses. *Science*, 346(6207):336–339, 2014.
- [27] P. M. Kraus, B. Mignolet, D. Baykusheva, A. Rupenyan, L. Horný, E. F. Penka, G. Grassi, O. I. Tolstikhin, J. Schneider, F. Jensen, L. B. Madsen, A. D. Bandrauk, F. Remacle, and H. J. Wörner. Measurement and laser control of attosecond charge migration in ionized iodoacetylene. *Science*, 350(6262):790–795, 2015.
- [28] Aaron von Conta, Andres Tehlar, Albert Schletter, Yasuki Arasaki, Kazuo Takatsuka, and Hans Jakob Wörner. Conical-intersection dynamics and ground-state chemistry probed by extreme-ultraviolet time-resolved photoelectron spectroscopy. *Nature communications*, 9(1):1–10, 2018.
- [29] F. Langer, C. P. Schmid, S. Schlauderer, M. Gmitra, J. Fabian, P. Nagler, C. Schüller, T. Korn, P. G. Hawkins, J. T. Steiner, U. Huttner, S. W. Koch, M. Kira, and R. Huber. Lightwave valleytronics in a monolayer of tungsten diselenide. *Nature*, 557(7703):76–80, May 2018.
- [30] Florian Siegrist, Julia A. Gessner, Marcus Ossiander, Christian Denker, Yi-Ping Chang, Malte C. Schröder, Alexander Guggenmos, Yang Cui, Jakob Walowski, Ulrike Martens, J. K. Dewhurst, Ulf Kleineberg, Markus Münzenberg, Sangeeta Sharma, and Martin Schultze. Light-wave dynamic control of magnetism. *Nature*, 571(7764):240–244, Jul 2019.
- [31] Peng Peng, Claude Marceau, and David M. Villeneuve. Attosecond imaging of molecules using high harmonic spectroscopy. *Nature Reviews Physics*, 1(2):144–155, Feb 2019.
- [32] Jonathan P. Marangos. Accessing the quantum spatial and temporal scales with x-fels. *Nature Reviews Physics*, 2(7):332–334, Jul 2020.
- [33] Kristina S. Zinchenko, Fernando Ardana-Lamas, Issaka Seidu, Simon P. Neville, Joscelyn van der Veen, Valentina Utrio Lanfaloni, Michael S. Schuurman, and Hans Jakob Wörner. Sub-7-femtosecond conical-intersection dynamics probed at the carbon k-edge. *Science*, 371(6528):489–494, 2021.
- [34] Marc Rebholz, Thomas Ding, Victor Despré, Lennart Aufleger, Maximilian Hartmann, Kristina Meyer, Veit Stooß, Alexander Magunia, David Wachs, Paul Birk, Yonghao Mi, Gergana Dimitrova Borisova, Carina da Costa Castanheira, Patrick Rupprecht, Georg Schmid, Kirsten Schnorr, Claus Dieter Schröter, Robert Moshhammer, Zhi-Heng Loh, Andrew R. Attar, Stephen R. Leone, Thomas Gaumnitz, Hans Jakob Wörner, Sebastian Rölling, Marco Butz, Helmut Zacharias, Stefan Düsterer, Rolf Treusch, Günter Brenner, Jonas Vester, Alexander I. Kuleff, Christian Ott, and Thomas Pfeifer. All-xuv pump-probe transient absorption spectroscopy of the structural molecular dynamics of di-iodomethane. *Phys. Rev. X*, 11:031001, Jul 2021.
- [35] D. Garratt, L. Misiekis, D. Wood, E. W. Larsen, M. Matthews, O. Alexander, P. Ye, S. Jarosch, C. Ferchaud, C. Strüber, A. S. Johnson, A. A. Bakulin, T. J. Penfold, and J. P. Marangos. Direct observation of ultrafast exciton localization in an organic semiconductor with soft x-ray transient absorption spectroscopy. *Nature Communications*, 13(1):3414, Jun 2022.
- [36] Erik P Månsson, Simone Latini, Fabio Covito, Vincent Wanie, Mara Galli, Enrico Peretto, Gianluca Stefanucci, Umberto De Giovannini, Mattea C Castrovilli, Andrea Trabattoni, Fabio Frassetto, Luca Poletto, Jason B Greenwood, François Légaré, Mauro Nisoli, Angel Rubio, and Francesca Calegari. Ultrafast dynamics of adenine following XUV ionization. *Journal of Physics: Photonics*, 4(3):034003, May 2022.
- [37] Gopal Dixit, Oriol Vendrell, and Robin Santra. Imaging electronic quantum motion with light. *Proceedings of*

- the National Academy of Sciences*, 109(29):11636–11640, 2012.
- [38] Daria Popova-Gorelova and Robin Santra. Imaging instantaneous electron flow with ultrafast resonant x-ray scattering. *Phys. Rev. B*, 91:184303, May 2015.
- [39] Daria Popova-Gorelova and Robin Santra. Imaging interatomic electron current in crystals with ultrafast resonant x-ray scattering. *Phys. Rev. B*, 92:184304, Nov 2015.
- [40] Maximilian Hollstein, Robin Santra, and Daniela Pfannkuche. Correlation-driven charge migration following double ionization and attosecond transient absorption spectroscopy. *Phys. Rev. A*, 95:053411, May 2017.
- [41] Victor Despré, Nikolay V. Golubev, and Alexander I. Kuleff. Charge migration in propiolic acid: A full quantum dynamical study. *Phys. Rev. Lett.*, 121:203002, Nov 2018.
- [42] Mingrui He, Yang Li, Yueming Zhou, Min Li, Wei Cao, and Peixiang Lu. Direct visualization of valence electron motion using strong-field photoelectron holography. *Phys. Rev. Lett.*, 120:133204, Mar 2018.
- [43] Kai-Jun Yuan and André D. Bandrauk. Ultrafast x-ray photoelectron imaging of attosecond electron dynamics in molecular coherent excitation. *The Journal of Physical Chemistry A*, 123(7):1328–1336, 2019. PMID: 30669842.
- [44] Ludger Inhester, Loren Greenman, Artem Rudenko, Daniel Rolles, and Robin Santra. Detecting coherent core-hole wave-packet dynamics in n₂ by time- and angle-resolved inner-shell photoelectron spectroscopy. *The Journal of Chemical Physics*, 151(5):054107, 2019.
- [45] Khadijeh Khalili, Ludger Inhester, Caroline Arnold, Anders S. Gertsen, Jens Wenzel Andreasen, and Robin Santra. Simulation of time-resolved x-ray absorption spectroscopy of ultrafast dynamics in particle-hole-excited 4-(2-thienyl)-2,1,3-benzothiadiazole. *Structural Dynamics*, 7(4):044101, 2020.
- [46] Stefano M. Cavaletto, Daniel Keefer, Jérémy R. Rouxel, Flavia Aleotti, Francesco Segatta, Marco Garavelli, and Shaul Mukamel. Unveiling the spatial distribution of molecular coherences at conical intersections by covariance x-ray diffraction signals. *Proceedings of the National Academy of Sciences*, 118(22):e2105046118, 2021.
- [47] François Mauger, Aderonke S. Folorunso, Kyle A. Hamer, Cristel Chandre, Mette B. Gaarde, Kenneth Lopata, and Kenneth J. Schafer. Charge migration and attosecond solitons in conjugated organic molecules. *Phys. Rev. Research*, 4:013073, Jan 2022.
- [48] Yeonsig Nam, Francesco Montorsi, Daniel Keefer, Stefano M. Cavaletto, Jin Yong Lee, Artur Nenov, Marco Garavelli, and Shaul Mukamel. Time-resolved optical pump-resonant x-ray probe spectroscopy of 4-thiouracil: A simulation study. *Journal of Chemical Theory and Computation*, 18(5):3075–3088, 2022. PMID: 35476905.
- [49] K. Chordiya, V. Despré, B. Nagyllés, F. Zeller, Z. Diveki, A. I. Kuleff, and M. U. Kahaly. Photo-ionization initiated differential ultrafast charge migration: Impact of molecular symmetries and tautomeric forms, 2022.
- [50] S. Yoo, B. Domercq, and B. Kippelen. Efficient thin-film organic solar cells based on pentacene/c60 heterojunctions. *Applied Physics Letters*, 85(22):5427–5429, 2004.
- [51] Karl Leo. Organic photovoltaics. *Nature Reviews Materials*, 1(8):1–2, 2016.
- [52] Anna Köhler and Heinz Bässler. *Electronic processes in organic semiconductors: An introduction*. John Wiley & Sons, 2015.
- [53] Francesca Fassioli, Rayomond Dinshaw, Paul C. Arpin, and Gregory D. Scholes. Photosynthetic light harvesting: excitons and coherence. *Journal of The Royal Society Interface*, 11(92):20130901, 2014.
- [54] Tammie R. Nelson, Dianelys Ondarse-Alvarez, Nicolas Oldani, Beatriz Rodriguez-Hernandez, Laura Alfonso-Hernandez, Johan F. Galindo, Valeria D. Kleiman, Sebastian Fernandez-Alberti, Adrian E. Roitberg, and Sergei Tretiak. Coherent exciton-vibrational dynamics and energy transfer in conjugated organics. *Nature Communications*, 9(1):2316, Jun 2018.
- [55] Shahnawaz Rafiq and Gregory D. Scholes. From fundamental theories to quantum coherences in electron transfer. *Journal of the American Chemical Society*, 141(2):708–722, Jan 2019.
- [56] L.S. Cederbaum and J. Zobeley. Ultrafast charge migration by electron correlation. *Chemical Physics Letters*, 307(3):205–210, 1999.
- [57] J. Breidbach and L. S. Cederbaum. Migration of holes: Formalism, mechanisms, and illustrative applications. *The Journal of Chemical Physics*, 118(9):3983–3996, 2003.
- [58] Alexander I. Kuleff, Siegfried Lünnemann, and Lorenz S. Cederbaum. Ultrafast charge migration following ionization in oligopeptides. In Paul Corkum, Sandro Silvestri, Keith A. Nelson, Eberhard Riedle, and Robert W. Schoenlein, editors, *Ultrafast Phenomena XVI*, pages 586–588, Berlin, Heidelberg, 2009. Springer Berlin Heidelberg.
- [59] Siegfried Lünnemann, Alexander I. Kuleff, and Lorenz S. Cederbaum. Charge migration following ionization in systems with chromophore-donor and amine-acceptor sites. *The Journal of Chemical Physics*, 129(10):104305, 2008.
- [60] Anthony D. Dutoi, Lorenz S. Cederbaum, Michael Wormit, Jan Hendrik Starcke, and Andreas Dreuw. Tracing molecular electronic excitation dynamics in real time and space. *The Journal of Chemical Physics*, 132(14):144302, 2010.
- [61] Anthony D. Dutoi, Michael Wormit, and Lorenz S. Cederbaum. Ultrafast charge separation driven by differential particle and hole mobilities. *The Journal of Chemical Physics*, 134(2):024303, 2011.
- [62] Anthony D. Dutoi and Lorenz S. Cederbaum. An excited electron avoiding a positive charge. *The Journal of Physical Chemistry Letters*, 2(18):2300–2303, 2011.
- [63] F. Remacle and R. D. Levine. Attosecond pumping of nonstationary electronic states of lih: Charge shake-up and electron density distortion. *Phys. Rev. A*, 83:013411, Jan 2011.
- [64] Alexander I Kuleff and Lorenz S Cederbaum. Ultrafast correlation-driven electron dynamics. *Journal of Physics B: Atomic, Molecular and Optical Physics*, 47(12):124002, jun 2014.
- [65] Hans Jakob Wörner, Christopher A. Arrell, Natalie Banerji, Andrea Cannizzo, Majed Chergui, Akshaya K. Das, Peter Hamm, Ursula Keller, Peter M. Kraus, Elisa Liberatore, Pablo Lopez-Tarifa, Matteo Lucchini, Markus Meuwly, Chris Milne, Jacques-E. Moser, Ursula Rothlisberger, Grigory Smolentsev, Joël Teuscher, Jeroen A. van Bokhoven, and Oliver Wenger. Charge migration and charge transfer in molecular systems. *Structural Dynamics*, 4(6):061508, 2017.

- [66] T. Kuś, B. Mignolet, R. D. Levine, and F. Remacle. Pump and probe of ultrafast charge reorganization in small peptides: A computational study through sudden ionizations. *The Journal of Physical Chemistry A*, 117(40):10513–10525, 2013. PMID: 24015765.
- [67] Albert Stolow, Arthur E. Bragg, and Daniel M. Neumark. Femtosecond time-resolved photoelectron spectroscopy. *Chemical Reviews*, 104(4):1719–1758, 2004. PMID: 15080710.
- [68] Kai-Jun Yuan, Chuan-Cun Shu, Daoyi Dong, and André D. Bandrauk. Attosecond dynamics of molecular electronic ring currents. *The Journal of Physical Chemistry Letters*, 8(10):2229–2235, 2017. PMID: 28468499.
- [69] A. Marciniak, V. Despré, V. Loriot, G. Karras, M. Hervé, L. Quintard, F. Catoire, C. Joblin, E. Constant, A. I. Kuleff, and F. Lépine. Electron correlation driven non-adiabatic relaxation in molecules excited by an ultrashort extreme ultraviolet pulse. *Nature Communications*, 10(1):337, Jan 2019.
- [70] Deependra Jadoun and Markus Kowalewski. Time-resolved photoelectron spectroscopy of conical intersections with attosecond pulse trains. *The Journal of Physical Chemistry Letters*, 12(33):8103–8108, 2021. PMID: 34410134.
- [71] Danielle Doweck and Piero Decleva. Trends in angle-resolved molecular photoelectron spectroscopy. *Phys. Chem. Chem. Phys.*, 24:24614–24654, 2022.
- [72] Stephan Hüfner. *Very high resolution photoelectron spectroscopy*, volume 715. Springer, 2007.
- [73] B. Mignolet, R. D. Levine, and F. Remacle. Localized electron dynamics in attosecond-pulse-excited molecular systems: Probing the time-dependent electron density by sudden photoionization. *Phys. Rev. A*, 86:053429, Nov 2012.
- [74] Aurelie Perveaux, David Lauvergnat, Fabien Gatti, Gábor J. Halász, Ágnes Vibók, and Benjamin Lasorne. Monitoring the birth of an electronic wavepacket in a molecule with attosecond time-resolved photoelectron spectroscopy. *The Journal of Physical Chemistry A*, 118(38):8773–8778, 2014. PMID: 25167166.
- [75] B Mignolet, R D Levine, and F Remacle. Charge migration in the bifunctional penna cation induced and probed by ultrafast ionization: a dynamical study. *Journal of Physics B: Atomic, Molecular and Optical Physics*, 47(12):124011, jun 2014.
- [76] Peter Puschnig, Stephen Berkebile, Alexander J. Fleming, Georg Koller, Konstantin Emtsev, Thomas Seyller, John D. Riley, Claudia Ambrosch-Draxl, Falko P. Netzer, and Michael G. Ramsey. Reconstruction of molecular orbital densities from photoemission data. *Science*, 326(5953):702–706, 2009.
- [77] P. Puschnig, E.-M. Reinisch, T. Ules, G. Koller, S. Soubatch, M. Ostler, L. Romaner, F. S. Tautz, C. Ambrosch-Draxl, and M. G. Ramsey. Orbital tomography: Deconvoluting photoemission spectra of organic molecules. *Phys. Rev. B*, 84:235427, Dec 2011.
- [78] B. Stadtmüller, M. Willenbockel, E. M. Reinisch, T. Ules, F. C. Bocquet, S. Soubatch, P. Puschnig, G. Koller, M. G. Ramsey, F. S. Tautz, and C. Kumpf. Orbital tomography for highly symmetric adsorbate systems. *EPL (Europhysics Letters)*, 100(2):26008, oct 2012.
- [79] Per Aake. Malmqvist, Alistair. Rendell, and Bjoern O. Roos. The restricted active space self-consistent-field method, implemented with a split graph unitary group approach. *The Journal of Physical Chemistry*, 94(14):5477–5482, 1990.
- [80] Francesco Aquilante, Jochen Autschbach, Rebecca K. Carlson, Liviu F. Chibotaru, Mickaël G. Delcey, Luca De Vico, Ignacio Fdez. Galván, Nicolas Ferré, Luis Manuel Frutos, Laura Gagliardi, Marco Garavelli, Angelo Giussani, Chad E. Hoyer, Giovanni Li Manni, Hans Lischka, Dongxia Ma, Per Åke Malmqvist, Thomas Müller, Artur Nenov, Massimo Olivucci, Thomas Bondo Pedersen, Daoling Peng, Felix Plasser, Ben Pritchard, Markus Reiher, Ivan Rivalta, Igor Schapiro, Javier Segarra-Martí, Michael Stenrup, Donald G. Truhlar, Liviu Ungur, Alessio Valentini, Steven Vancocillie, Valera Veryazov, Victor P. Vysotskiy, Oliver Weingart, Felipe Zapata, and Roland Lindh. Molcas 8: New capabilities for multiconfigurational quantum chemical calculations across the periodic table. *Journal of Computational Chemistry*, 37(5):506–541, 2016.
- [81] Thom H. Dunning. Gaussian basis sets for use in correlated molecular calculations. i. the atoms boron through neon and hydrogen. *The Journal of Chemical Physics*, 90(2):1007–1023, 1989.
- [82] Benjamin P. Pritchard, Doaa Altarawy, Brett Didier, Tara D. Gibson, and Theresa L. Windus. New basis set exchange: An open, up-to-date resource for the molecular sciences community. *Journal of Chemical Information and Modeling*, 59(11):4814–4820, 2019. PMID: 31600445.
- [83] E Heinecke, D Hartmann, R Müller, and A Hese. Laser spectroscopy of free pentacene molecules (i): The rotational structure of the vibrationless $s_1 \leftarrow s_0$ transition. *The Journal of chemical physics*, 109(3):906–911, 1998.
- [84] Stefan Grimme and Maja Parac. Substantial errors from time-dependent density functional theory for the calculation of excited states of large π systems. *ChemPhysChem*, 4(3):292–295, 2003.
- [85] Pedro B. Coto, Sahar Sharifzadeh, Jeffrey B. Neaton, and Michael Thoss. Low-lying electronic excited states of pentacene oligomers: A comparative electronic structure study in the context of singlet fission. *Journal of Chemical Theory and Computation*, 11(1):147–156, Jan 2015.
- [86] Goran Kovačević and Valera Veryazov. Luscus: molecular viewer and editor for molcas. *Journal of cheminformatics*, 7(1):1–10, 2015.
- [87] Koichi Momma and Fujio Izumi. VESTA3 for three-dimensional visualization of crystal, volumetric and morphology data. *Journal of Applied Crystallography*, 44(6):1272–1276, 2011.
- [88] Daria Popova-Gorelova. Imaging electron dynamics with ultrashort light pulses: A theory perspective. *Applied Sciences*, 8(3), 2018.
- [89] Caroline Arnold, Oriol Vendrell, and Robin Santra. Electronic decoherence following photoionization: Full quantum-dynamical treatment of the influence of nuclear motion. *Phys. Rev. A*, 95:033425, Mar 2017.
- [90] Danylo T. Matselyukh, Victor Despré, Nikolay V. Golubev, Alexander I. Kuleff, and Hans Jakob Wörner. Decoherence and revival in attosecond charge migration driven by non-adiabatic dynamics. *Nature Physics*, 18(10):1206–1213, Oct 2022.
- [91] Andrew J. Jenkins, Morgane Vacher, Rebecca M. Twidale, Michael J. Bearpark, and Michael A. Robb. Charge migration in polycyclic norbornadiene cations:

- Winning the race against decoherence. *The Journal of Chemical Physics*, 145(16):164103, 2016.
- [92] V. Despré, A. Marciniak, V. Lorient, M. C. E. Galbraith, A. Rouzée, M. J. J. Vrakking, F. Lépine, and A. I. Kuleff. Attosecond hole migration in benzene molecules surviving nuclear motion. *The Journal of Physical Chemistry Letters*, 6(3):426–431, 2015. PMID: 26261959.